

Experimental Study of Fracture Propagation Mechanisms by Oriented Perforation Technology for SRV Fracturing

CHANG Xin^{[a],*}; WANG Huaidong^[a]; CHENG Yuanfang^[a]; HAN Xiuting^[a]

^[a] School of Petroleum Engineering, China University of Petroleum (East China), Qingdao, China.

*Corresponding author.

Supported by the National Natural Science Foundation of China (51574270).

Received 30 September 2015; accepted 4 November 2015
Published online 31 December 2015

Abstract

Due to the growing importance of shale oil and gas resources, more effective techniques to develop unconventional reservoirs are strongly required. In this paper, a new volumetric fracturing measure for unconventional resources based on oriented perforation technology has been introduced. Moreover, this innovative approach was validated through a series of laboratory experiments varying the parameters of physical models, such as perforation azimuth, perforation length and horizontal stress difference. The results showed that the artificial hydraulic fracture formed by using oriented perforation technology was not a satisfactory straight dual-wing fracture, instead, it was a bent dual-wing crack like “S” or “X”, which could significantly increase the stimulated reservoir volume. The perforation azimuth and horizontal stress difference were the primary factors that affected the formation of multi fractures. The reorientation path was extended with the increasing of the oriented perforation azimuth angle, but decreased with the increasing of horizontal stress difference. In addition, increasing the perforation length could greatly decrease the initiation pressure. Therefore, the oriented perforation technology could be as a powerful way to accelerate the exploitation of the unconventional reservoirs.

Key words: Unconventional reservoir; Stimulated reservoir volume; Oriented perforation technology; Fracture propagation mechanisms; Perforation azimuth; Horizontal stress difference

Chang, X., Wang, H. D., Cheng, Y. F., & Han, X. T. (2015). Experimental study of fracture propagation mechanisms by oriented perforation technology for SRV fracturing. *Advances in Petroleum Exploration and Development*, 10(2), 44-49. Available from: URL: <http://www.cscanada.net/index.php/aped/article/view/7621> DOI: <http://dx.doi.org/10.3968/7621>

INTRODUCTION

Hydraulic fracturing is a widely used technology in extracting hydrocarbon from ultra-low permeability unconventional reservoirs such as shale and tight gas sand^[1-2]. A primary goal in unconventional reservoirs is to contact as much rock as possible with a fracture or a fracture network of appropriate conductivity^[3]. Generally, hydraulic fracturing is seen as creating a single, planar, opening mode tensile fracture. But in low-matrix-permeability applications, such as hydrocarbon production from shale or tight gas sand, the process of hydraulic stimulation has been conceptualized as creating a complex network^[4-5]. Referring to the successful practice of North America, the complex fracture network is typically accomplished by drilling horizontal wells and placing multiple transverse fractures along the lateral. However, there are still many low permeable and unconventional reservoirs in china, especially in Changqing, Xinjiang, Jilin, and so forth, can't be developed effectively as a result of their unique geomechanical characteristics^[6-8]. Therefore, it is crucial to find another approach to deal with this kind of reservoir.

In this paper, a new volumetric fracturing measure for unconventional resources based on oriented perforation technology has been introduced. Firstly, this innovative approach was validated through theoretical analysis. Then, a series of tests were designed to study the influencing factors on the initial fracture position and pattern of artificial hydraulic fractures with oriented perforating by the large-scale real tri-axial hydraulic fracturing physical simulation experiment system.

1. MATHEMATICAL MODEL

1.1 Fracture Initiation Pressure of Oriented Perforation Technology

During hydraulic fracturing, the rock around the wellbore is under complex stress conditions, as a result of the fluid pressure, the in situ stress, the pore pressure, the additional stress caused by infiltration of fracturing fluid, and so on^[9]. For simplicity, in this paper the rock is assumed as a homogeneous, isotropic, and linear elastic porous material, and the stress distribution around the wellbore is considered as a plane strain problem. Moreover, the sign of compression stress is assumed as negative and the tensile stress is assumed as positive.

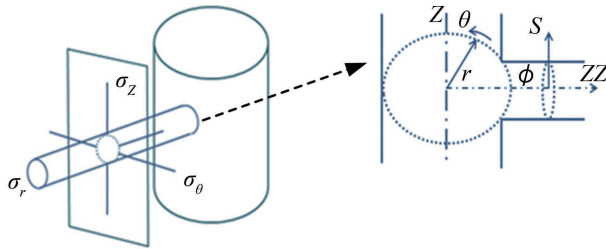


Figure 1
Stress Distribution Around the Perforation Hole

The perforation hole is assumed as a cylindrical micro-hole perpendicular to the borehole axis, and the stress distribution around the perforation hole in the cylindrical coordinate system (Figure 1), are expressed in Equation (1):

$$\begin{cases} \sigma_s = \frac{\sigma_\theta + \sigma_z}{2} \left(1 - \frac{r_{hs}^2}{s^2}\right) + \frac{\sigma_\theta - \sigma_z}{2} \left(1 + \frac{3r_{hs}^4}{s^4} - \frac{4r_{hs}^2}{s^2}\right) \cos 2\phi - \frac{r_{hs}^2}{s^2} P_{pf} \\ \sigma_\phi = \frac{\sigma_\theta + \sigma_z}{2} \left(1 + \frac{r_{hs}^2}{s^2}\right) - \frac{\sigma_\theta - \sigma_z}{2} \left(1 + \frac{3r_{hs}^4}{s^4}\right) \cos 2\phi + \frac{r_{hs}^2}{s^2} P_{pf} \\ \sigma_{zz} = \sigma_r - 2\nu(\sigma_\theta - \sigma_z) \frac{r_{hs}^2}{s^2} \cos 2\phi \\ \tau_{s\phi} = \frac{\sigma_\theta - \sigma_z}{2} \left(1 - \frac{3r_{hs}^4}{s^4} + \frac{2r_{hs}^2}{s^2}\right) \sin 2\phi \\ \tau_{s\phi} = \tau_{sz} = 0 \end{cases} \quad (1)$$

Where σ_θ is the tangential or hoop stress around the wellbore, MPa; σ_r is the radial stress and σ_z is the axial stress along the wellbore, MPa; σ_ϕ is the hoop stress around the perforation hole, MPa; σ_s is the radial stress and σ_{zz} is the axial stress along the perforation hole, MPa; $\tau_{s\phi}$, $\tau_{z\phi}$, τ_{sz} are corresponding shear stress, MPa; P_{pf} is the hydraulic fracturing fluid pressure, MPa; r_{hs} is the radius of the perforation hole, m; s is the distance from the centre of the perforation hole, m; θ is the wellbore circumferential angle starting from the maximum horizontal principal stress; ϕ is the perforation hole circumferential angle starting from the σ_θ using the right-hand rule.

According to the linear elastic fracture mechanics (LEFM), the hydraulic fracture initiates when the maximum principal stress in the θ' direction reaches the rock tensile strength, which can be written as

$$\sigma(\theta') = T \quad (2)$$

Where T is the rock tensile strength, MPa.

Given the stress distributions around the perforation hole, the maximum principal stresses can be obtained by

$$\sigma_{\max}(\theta') = \frac{\sigma_\phi + \sigma_{zz}}{2} + \sqrt{\left(\frac{\sigma_\phi - \sigma_{zz}}{2}\right)^2 + \tau_{z\phi}^2} \quad (3)$$

Substituting Equation (3) to (2), and considering the permeability of the wellbore, the fracture initiation pressure of OPT can be achieved by

$$\sigma_{\max}(\theta') - \alpha P_0 = T \quad (4)$$

Where α is the Boit coefficient, P_0 is the in-situ pore Pressure, MPa.

1.2 Feasibility Studies of Creating Complex Fracture Network by OPT

In order to validate the feasibility of creating complex fracture network by oriented perforation technology, taking well QP2 in Changqing oilfield for case study. The well parameters listed in Table 1, and the stresses distribution at the heel of the perforation hole were computed, as shown in Figures 2 and 3.

Table 1
Parameters of Well QP2 in Changqing Oilfield

Parameters	Value
Wellbore diameter (m)	0.1
well depth (m)	3,100.0
Well deviation	0°
Well azimuth	0°
Perforation hole diameter (m)	0.06
In-situ stresses (MPa)	42.01, 35.95, 29.02
Elastic modulus of rock (MPa)	32,500.0
Poisson's ratio of rock	0.2
Pore pressure (MPa)	18.0
Fracturing fluid pressure (MPa)	20.0, 30.0
Biot coefficient	0.65
Perforation length (m)	1.0
Rock tensile strength (MPa)	2.0

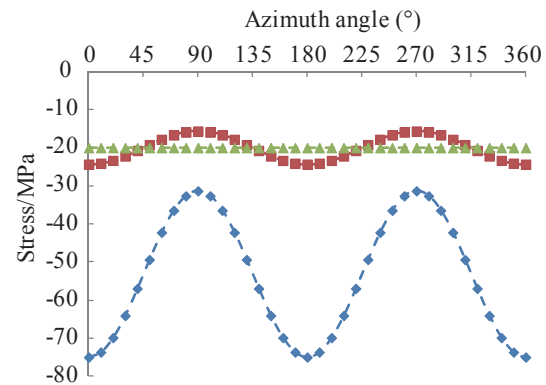


Figure 2
Stress Distribution Around the Perforation Hole When $P_{pf} = 20$ MPa

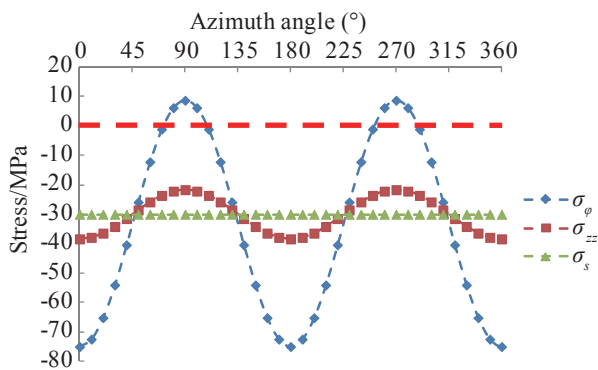


Figure 3
Stress Distribution Around the Perforation Hole When $P_{pf} = 30$ MPa

As can be seen in Figures 2 and 3, when the perforation azimuth angle is fixed ($\theta = 0^\circ$), the maximum stresses around the perforation hole periodically appeared at $\phi = 90^\circ, 270^\circ$. Meanwhile, as the fracturing fluid pressure increase from 20 MPa to 30 MPa, the maximum stress is changing from the compressive stress into tensile stress. Therefore, the breakdown may firstly occur at the top and bottom surface of the perforation hole, and in the calculation of initiation pressure, only $\phi = 90^\circ$ is taken to use.

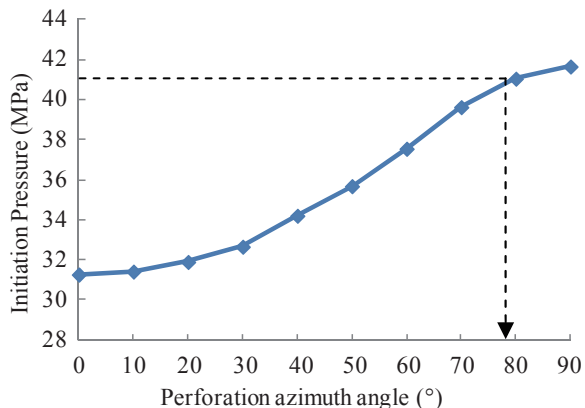


Figure 4
Fracture Initiation Pressure Changes With the Perforation Azimuth Angle

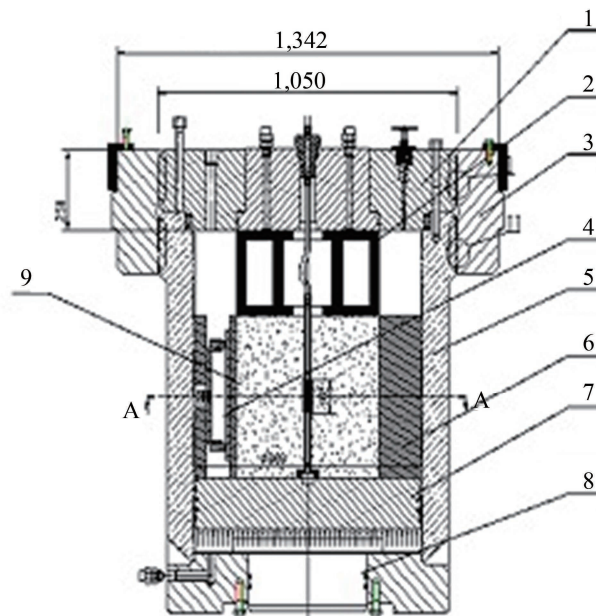
It is obvious in Figure 4 that the fracture initiation pressure increases as the perforation azimuth angle increases. Moreover, according to the calculation results, when the perforation azimuth angle, the fracture initiation pressure is bigger than that of the open hole model (41.41 MPa). So it means that increasing the perforation azimuth angle can form multiple initiation sites along the perforation hole, and then induced the formation to generate a fracture network.

2. EXPERIMENTAL DEVICE AND EXPERIMENTAL PARAMETERS SELECTION

2.1 Experimental Device

The Experiments were conducted by using a large-scale real tri-axial hydraulic fracturing physical simulation

experiment system, which is mainly composed of five parts: Tri-axial high pressure cylinder (Figure 5), servo control system, hydraulic pump, master controlling computer and signal acquisition unit. The horizontal principal stresses were generated by the four hydraulic jacks around the synthetic rock specimens, and the vertical stress was loaded by the crane underneath the sample. The maximum pressure is up to 60 MPa. The hydraulic fluid injection pressure is controlled by a servo hydraulic pump of ATW-1000, with a maximum capacity of fluid injection pressure of 80 MPa.



1-Cylinder head; 2-Press cake; 3-Clamp; 4-Confining pressure cylinder; 5-Cylinder block; 6-Heel block; 7-Piston; 8-Sealing element; 9-Sample assembly

Figure 5
Structure Diagram of Tri-Axial High Pressure Cylinder

2.2 Sample Preparation

Concrete sample made of Portland cement (No. 325) and fine-sand (120 mesh) with the proportion of 1:1 were used as analogs of the formation rock. The cement blocks used in the experiments were cubes of 0.1 m on a side. While the sample was produced, a steel tube with an inside diameter of 8 mm was put in the center of the block by pouring the cement around it to simulate a wellbore with a depth of 60 mm, and three plastic pipes with an inside diameter of 2.5 mm were used to simulate the perforation hole. A generalized view of the sample is presented in Figure 6. The geomechanical properties of cement blocks are shown in Table 2.

2.3 Experimental Parameters

According to the scaling laws, a series of 10 laboratory hydraulic fracturing tests were conducted in a normal-faulting stress regime to investigate the initial fracture position and pattern of artificial hydraulic fractures with oriented perforating. The constant value of Vertical stress

was 24 MPa. In this experiment, guar gum fracturing fluid with a viscosity of 52.4 mPa·s was injected at a constant flow rate of 4.1×10^{-9} m³/s. At the same time, a blue dye was also added into the fluid to allow better tracing of the hydraulic fracture. Detailed experimental parameters are shown in Table 3.

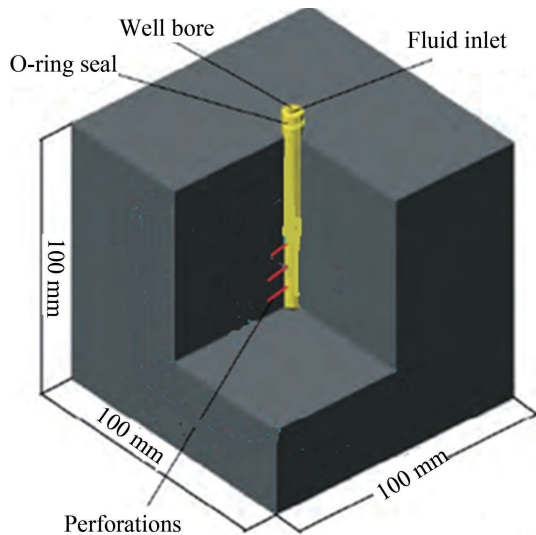


Figure 6
Schematic of the Rock Sample

Table 2
Geomechanical Properties of Cement Blocks

Parameters	Value
Elastic modulus of rock (MPa)	8,763.00
Poisson's ratio of rock	0.23
Unconfined compressive strength (MPa)	25.46
Tensile strength (MPa)	2.34
Permeability (mD)	0.12
Porosity (%)	2.06

Table 3
Experiment Parameters for Oriented Hydraulic Fracturing Tests

Sample No.	Perforation azimuth angle θ (°)	σ_H /MPa	σ_h /MPa	Perforation length/mm
#1	0	20	14	20
#2	30	20	14	20
#3	45	20	14	20
#4	60	20	14	20
#5	90	20	14	20
#6	0	20	14	5
#7	0	20	14	10
#8	0	20	14	15
#9	45	18	14	20
#10	45	16	14	20

3. EXPERIMENTAL RESULTS AND ANALYSIS

3.1 Perforation Azimuth Angle

In this paper, five hydraulic fracturing tests were conducted on cement blocks to investigate the influence of perforation azimuth angle on fracture initiation pressure and geometry. The experimental results are presented in Table 4. And, photographs taken from each block sample are shown in Figure 7.

Table 4
Experimental Results of OPT With Different Perforation Azimuth Angle

Sample No.	Perforation azimuth angle θ (°)	Initiation pressure/MPa	Reorientation path/cm	Fracture geometry
#1	0	18.96	---	Planar fracture
#2	30	20.22	2.51	Tortuous fracture
#3	45	21.64	2.77	Tortuous fracture
#4	60	23.48	3.16	Multiple fractures
#5	90	19.06	---	Planar fracture

As indicated in Table 4, the perforation azimuth angle has an important effect on fracture initiation pressure and reorientation path. With the increasing of azimuth angle, fracture initiation pressure and reorientation path are both rapidly increasing. For sample No. 1, the perforation azimuth angle is 0°, a typical single planar fracture is created and propagating in the direction of the maximum horizontal stress. As the deviation of the perforation direction from the direction of the maximum horizontal principal stress continues to rise, the geometry becomes more and more complex. For sample No. 2 and sample No. 3, "S" type tortuous fracture are formed. When the perforation azimuth angle is 60°, "X" type multi-fractures are formed, which can greatly increase the stimulated reservoir volume. However, when the perforation azimuth angle increases to 90°, the fracture is no longer initiating along the perforation hole, instead, it crosses the micro-annulus and then turn to the direction of the maximum horizontal stress.

From the above experimental results, the geometries of fractures propagation with different perforation azimuth angle can be classified into four categories, as shown in Figure 8.

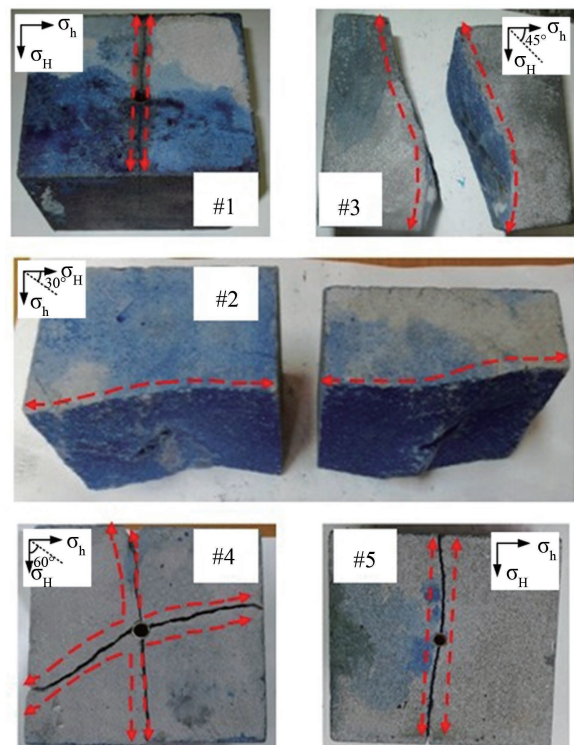


Figure 7
Geometry of Fracture Propagation

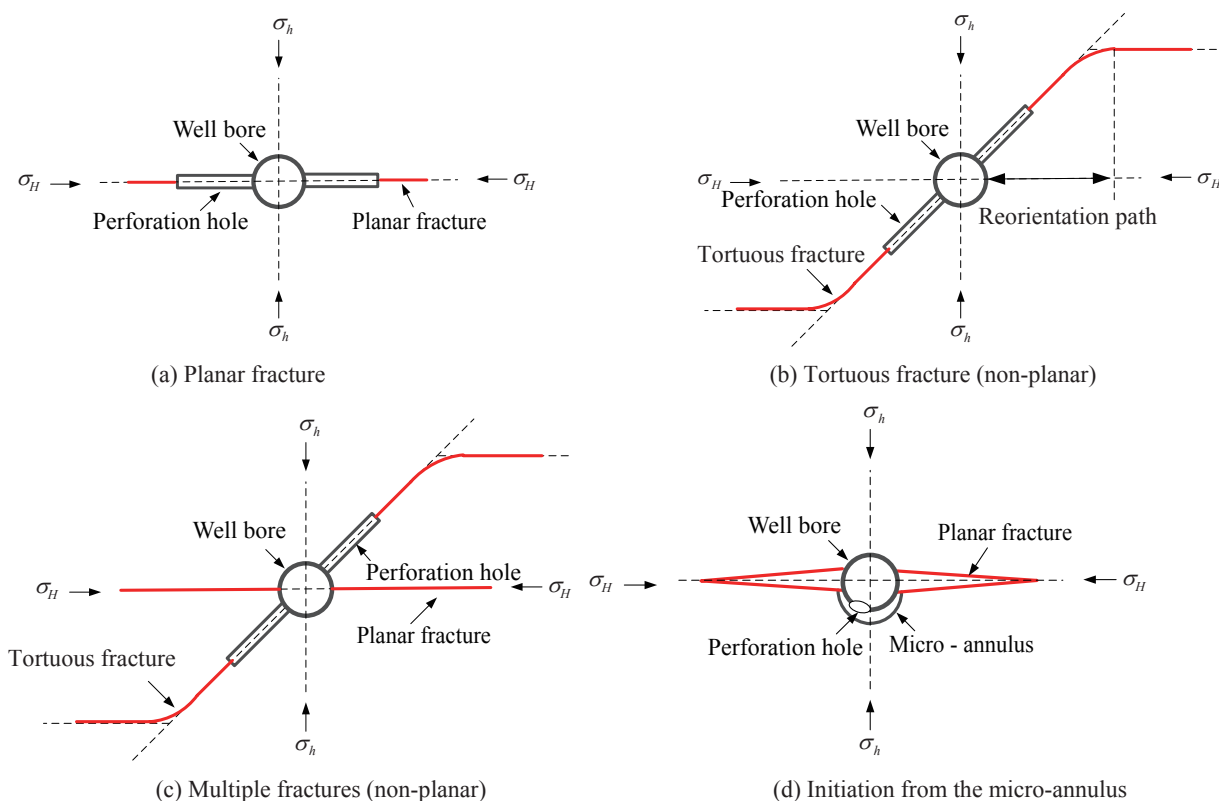


Figure 8
Geometry of Fracture Propagation With Different Perforation Azimuth Angle

3.2 Horizontal Stress Difference

In order to reveal the influence of horizontal stress difference on fracture initiation pressure and geometry, three hydraulic fracturing tests were conducted. The experimental results are shown in Table 5.

Table 5
Experimental Results of OPT With Different Horizontal Stress Difference

Sample No.	σ_H /MPa	σ_h /MPa	Initiation pressure/MPa	Reorientation path/cm
#3	20	14	21.64	2.77
#9	18	14	22.26	3.92
#10	16	14	23.01	4.57

As can be seen from Table 5, with the horizontal stress difference decreased, the fracture initiation pressure and reorientation path increased significantly. It means that when the oriented perforation technology was taken in lower horizontal stress contrast reservoir, the induced fracture can contact as much rock as possible, thus realizes the improvement of fracturing stimulation.

3.3 Perforation Length

In order to reveal the influence of perforation length on fracture initiation pressure and geometry, four hydraulic fracturing tests were conducted. The experimental results are shown in Table 6.

Table 6
Experimental Results of OPT With Different Perforation Length

Sample No.	Perforation length/mm	Initiation pressure/MPa	Fracture geometry
#6	5	20.82	Planar fracture
#7	10	20.08	Planar fracture
#8	15	19.34	Planar fracture
#1	20	18.96	Planar fracture

It is obvious in Table 6 that the fracture initiation pressure decreases dramatically as the perforation length increases. The reason for this phenomenon is that more high pressure fluid can directly act on the rock surface and then force the fracture initiation. This finding is very useful for OPT oilfield application.

CONCLUSION

The following conclusions can be drawn as the results of this study:

(a) During oriented perforating fracturing, multiple fracture initiation sites along the perforation hole could be formed by manual. And the fracture geometry was not a satisfactory straight dual-wing fracture, instead, it was a bent dual-wing crack like “S” or “X”, which could significantly increase the SRV, thus realized the improvement of fracturing stimulation.

(b) With the increasing of the perforation azimuth angle, the fracture initiation pressure and reorientation path were all extended, but decreased with the increasing of horizontal stress difference. Moreover, the fracture initiation pressure could decrease dramatically as the perforation length increased.

REFERENCES

- [1] Weng, D. W., Lei, Q., Xu, Y., Li, Y., Li, D. Q., & Wang, W. X. (2011). Network fracturing techniques and its application in the field. *Acta Petrolei Sinica*, 32(2), 280-284.
- [2] Wang, H., Liao, X. W., Zhao, X. L., Zhao, D. F., & Liao, C. L. (2014). The progress of reservoir stimulation simulation technology in unconventional oil and gas reservoir. *Special Oil and Gas Reservoirs*, 21(2), 8-15.
- [3] Hu, Y. Q., Jia, S. G., Zhao, J. Z., Zhang Y., & Mi, Q. B. (2013). Study on controlling conditions in network hydraulic fracturing. *Journal of Southwest Petroleum University (Science & Technology Edition)*, 35(4), 126-132.
- [4] Warpinski, N., Mayerhofer, M., & Vincent, M. (2008). *Stimulating unconventional reservoirs: Maximizing network growth while optimizing fracture conductivity*. Paper presented at the SPE Unconventional Resources Conference, Keystone, Colorado, USA.
- [5] Wu, Q., Xu, Y., Wang, X. Q., Wang, T. F., & Zhang, S. L. (2012). Volume fracturing technology of unconventional reservoirs: Connotation, design optimization and implementation. *Petroleum Exploration and Development*, 39(3), 377-384.
- [6] Zhang, G. Q., & Chen, M. (2009). Complex fracture shapes in hydraulic fracturing with oriented perforations. *Petroleum Exploration and Development*, 36(1), 103-107.
- [7] Jiang, H., Chen, M., Zhang, G. Q., Jin, Y., Zhao, Z. F., & Zhu, G. F. (2009). Impact of oriented perforation on hydraulic fracture initiation and propagation. *Chinese Journal of Rock Mechanics and Engineering*, 28(7), 1321-1326.
- [8] Tang, M. R., Zhao, Z. F., Li, X. W., & Zhao, W. (2010). Study and test on the new technology of multi-fracture fracturing. *Oil Drilling & Production Technology*, 32(2), 71-74.
- [9] Zhu, H. Y., Deng, J. G., Jin, X. C., Hu, L. B., & Luo, B. (2015). Hydraulic fracture initiation and propagation from wellbore with oriented perforation. *Rock Mechanics and Rock Engineering*, 48(2), 585-601.